The 14th International Topical Meeting on Nuclear Reactor Thermalhydraulics, NURETH-14
Toronto, Ontario, Canada, September 25-30, 2011

NURETH14-274

NUMERICAL PREDICTIONS OF BUBBLY TWO-PHASE FLOWS WITH OPENFOAM

E. Michta[1], K. Fu[1], H. Anglart[1] and K. Angele[2]
[1] Royal Institute of Technology (KTH), Stockholm, Sweden
[2] Vattenfall Research and Development AB, Stockholm, Sweden

Abstract

A new model for simulation of bubbly two-phase flows has been developed and implemented into an open-source Computational Fluid Dynamics (CFD) code OpenFOAM. The model employs the two-fluid framework with closure relationships for the interfacial momentum transfer. The bubble size is calculated based on the solution of the interfacial area concentration equations. The predictions are validated against a wide range of experimental data containing measured void fraction, the phasic velocity and the interfacial area concentration. The new model demonstrates the ability to capture the wall peaking of void fraction for small bubbles. The predicted levels of void fraction and phasic velocities are in good agreement with measured data.

Introduction

Simulations and modelling of turbulent two-phase flows and heat transfer remain one of the major challenges in prediction of the over-all performance and safety features of Light Water Reactors (LWR). In particular, predictions of the onset of heat transfer crisis, either of the Departure from Nucleate Boiling (DNB) or the dryout type require adequate resolution of the flow field, including the underlying turbulence structure. In two-phase flows both the flow field and the turbulent structure are intimately coupled to the behaviour of the interface between the two phases. Clearly, a complete two-phase flow model has to take into account these factors and provide proper closure relationships to the governing conservation equations.

The goal of the present work is to implement and validate a two-phase bubbly flow model using the OpenFOAM framework [1]. Unlike commercial CFD codes, OpenFOAM provides a complete access to the source code, enabling a full control over the implemented models. Thanks to its object-oriented structure, OpenFOAM can accommodate various optional sub-models without a necessity of re-writing the code. This is a particularly important feature for the modelling of two-phase flows, where several equivalent formulations of closure laws need to be tested.

1. Governing equations

The current model employs the two-fluid formulation of the two-phase flow [2,3]. For adiabatic bubbly two phase flows, the conservation equations are as follows,

$$\frac{\partial \alpha_k}{\partial t} + \nabla \cdot \left(\alpha_k \vec{U}_k \right) = 0 \tag{1}$$

$$\frac{\partial \alpha_k \vec{U}_k}{\partial t} + \nabla \cdot \left(\alpha_k \vec{U}_k \vec{U}_k\right) = -\nabla \cdot \left[\alpha_k \left(\overline{R}_k + \overline{R}_k^t\right)\right] - \frac{\alpha_k}{\rho_k} \nabla p + \alpha_k \vec{g} + \frac{\vec{M}_k}{\rho_k} \tag{2}$$

Here α_k is the volume fraction, $\vec{U}_k$ is the velocity vector, ρ_k is the density, p is the pressure, t is the time, $\vec{g}$ is the gravity vector and k is the phase index. In writing Eqs. (1) and (2) it is assumed that both phases are incompressible and that they share the same pressure field. The total effective stress tensor is modelled using the Boussinesq approximation as follows,

$$\overline{R}_k^{eff} \equiv \overline{R}_k + \overline{R}_k^t = -\left(\nu_k + \nu_k^t\right)\left[\nabla \vec{U}_k + \left(\nabla \vec{U}_k\right)^T - \frac{3}{2}\bar{I}\nabla \cdot \vec{U}_k\right] + \frac{3}{2}\bar{I}k_k \tag{3}$$

where ν_k is the molecular kinematic viscosity of phase k, ν_k^t is the turbulent kinematic viscosity of phase k, k_k is the turbulent kinetic energy of phase k and $\bar{I}$ denotes a unit tensor.

1.1 Interfacial forces

For bubbly two-phase flows, interfacial forces can be express as a superposition of various forces exerted by the continuous liquid phase ($k = l$) on the disperse gas phase ($k = g$):

$$\vec{M}_g = \vec{M}_g^D + \vec{M}_g^L + \vec{M}_g^{WL} + \vec{M}_g^{TD} + \vec{M}_g^{VM} . \tag{4}$$

The force exerted by bubbles on the liquid phase is then obtained as,

$$\vec{M}_l = -\vec{M}_g \quad . \tag{5}$$

The drag force is modelled using the Ishii-Zuber correlation for the drag coefficient [4]:

$$\vec{M}_g^D = -\frac{3}{4}\frac{C_D}{D_S}\rho_l \alpha \left\|\vec{U}_g - \vec{U}_l\right\|\left(\vec{U}_g - \vec{U}_l\right), \tag{6}$$

where D_S is the Sauter mean diameter of bubbles and C_D is the drag coefficient found as,

$$C_D = \max\left(24\frac{1+0.15\,\mathrm{Re}_b^{0.687}}{\mathrm{Re}_b}, 0.44\right) , \tag{7}$$

$$\mathrm{Re}_b = \frac{\rho_l \left\|\vec{U}_g - \vec{U}_l\right\| D_S}{\mu_m}, \tag{8}$$

$$\mu_m = \mu_l \left(1 - \frac{\alpha}{\alpha_{\max}}\right)^{-2.5\alpha_{\max}\mu^*} , \tag{9}$$

where $\alpha_{\max}$ is the void fraction at maximum packing equal to 0.52 and:

$$\mu^* = \frac{\mu_g + 0.4\mu_l}{\mu_g + \mu_l}. \tag{10}$$

The lift force is modelled as follows [5],

$$\vec{M}_g^L = C_L \rho_l \alpha \left(\vec{U}_g - \vec{U}_l\right) \times \nabla \times \vec{U}_l, \tag{11}$$

where the lift coefficient is taken as [6],

$$C_L = \begin{cases} \min\left[0.288\tanh\left(0.121\mathrm{Re}_b\right), f\left(\mathrm{Eo}_\mathrm{d}\right)\right] & \text{if} \quad \mathrm{Eo}_\mathrm{d} < 4 \\ f\left(\mathrm{Eo}_\mathrm{d}\right) & \text{if} \quad 4 \le \mathrm{Eo}_\mathrm{d} \le 10 \\ -0.27 & \text{if} \quad \mathrm{Eo}_\mathrm{d} > 10 \end{cases}, \tag{12}$$

$$f\left(\mathrm{Eo}_\mathrm{d}\right) = 0.001509\mathrm{Eo}_\mathrm{d}^3 - 0.0159\mathrm{Eo}_\mathrm{d}^2 - 0.0204\mathrm{Eo}_\mathrm{d} + 0.474 \quad . \tag{13}$$

Here,

$$\mathrm{Eo}_\mathrm{d} = \frac{g\left(\rho_l - \rho_g\right)d_h}{\sigma}, \tag{14}$$

where,

$$\mathrm{d}_h = D_S\left(1 + 0.163\mathrm{Eo}^{0.757}\right)^{1/3}, \tag{15}$$

and,

$$\mathrm{Eo} = \frac{g\left(\rho_l - \rho_g\right)D_S^2}{\sigma}. \tag{16}$$

The wall lubrication force for bubbly two-phase flow in a pipe is given as [6],

$$\vec{M}_g^{WL} = \frac{1}{2} C_{WL} \rho_l \alpha D_S \left[\frac{1}{y^2} - \frac{1}{(D-y)^2}\right] \left\| \left(\vec{U}_g - \vec{U}_l\right) \cdot \vec{x} \right\|^2 \vec{n}_w, \tag{17}$$

where D is the pipe diameter, y is a distance to the wall, $\vec{x}$ is the axial direction and $\vec{n}_w$ is the normal to the wall pointing towards the fluid. The lubrication force coefficient is given as,

$$C_{WL} = \begin{cases} 0.47 & \text{if} \quad \mathrm{Eo} < 1 \\ \mathrm{e}^{-0.933\mathrm{Eo}+0.179} & \text{if} \quad 1 \le \mathrm{Eo} \le 5 \\ 0.00599\mathrm{Eo} - 0.0187 & \text{if} \quad 5 \le \mathrm{Eo} \le 33 \\ 0.179 & \text{if} \quad 33 < \mathrm{Eo} \end{cases}. \tag{18}$$

The turbulent dispersion force is given as [7],

$$\vec{M}_g^{TD} = -\frac{3}{4}\frac{C_D}{D_S}\frac{\nu_l^t}{\mathrm{Pr}_l^t}\rho_l\left\|\vec{U}_g - \vec{U}_l\right\|\vec{\nabla}\alpha. \tag{19}$$

The virtual mass force is calculated as [8],

$$\vec{M}_g^{VM} = -\frac{1}{2}\rho_l\frac{1+2\alpha}{1-\alpha}\left(\frac{D\vec{U}_g}{Dt} - \frac{D\vec{U}_l}{Dt}\right), \tag{20}$$

where $D/Dt = \partial/\partial t + \vec{U}\cdot\nabla$ is the total derivative.

1.2 Interfacial area concentration transport equations

The spatial and temporal evolution of the interfacial area concentration is described with the following transport equation [9],

$$\frac{\partial a_i}{\partial t} + \nabla\cdot\left(a_i\vec{U}_g\right) = 12\pi\left(\frac{\alpha}{a_i}\right)^2\left(\phi_n^{CO} + \phi_n^{BK}\right), \tag{21}$$

where ϕ_n^{CO} and ϕ_n^{BK} are the sinks and sources of the interfacial area due to the coalescence and break-up, respectively. These terms can be calculated as [9],

$$\phi_n^{CO} = -\Gamma_C\frac{\alpha^2\varepsilon_l^{1/3}}{D_S^{1/3}\left(\alpha_{\max}-\alpha\right)}\exp\left(-K_C\frac{D_S^{11/3}\rho_l^{1/2}\varepsilon_l^{1/3}}{\sigma^{1/2}}\right),\ \Gamma_C = 0.005,\ K_C = 1.29, \tag{22}$$

and

$$\phi_n^{BK} = \Gamma_B\frac{\alpha(1-\alpha)\varepsilon_l^{1/3}}{D_S^{1/3}\left(\alpha_{\max}-\alpha\right)}\exp\left(-K_B\frac{\sigma}{D_S^{5/3}\rho_l\,\varepsilon_l^{2/3}}\right),\ \Gamma_B = 0.007,\ K_B = 1.37\ . \tag{23}$$

Here ε_l is the turbulent energy dissipation of the liquid phase. Another formulation of the terms has been proposed in [10],

$$\phi_n^{CO} = -K_{C1}\frac{\alpha^2\varepsilon_l^{1/3}\exp\left(-K_{C3}\dfrac{\mathrm{We}}{\mathrm{We}_{cr}}\right)}{D_S^{11/3}\left[\left(\dfrac{\alpha_{\max}^{1/3}-\alpha^{1/3}}{\alpha_{\max}^{1/3}}\right)+K_{C2}\alpha\sqrt{\dfrac{\mathrm{We}}{\mathrm{We}_{cr}}}\right]},\quad \begin{cases} K_{C1} = 2.86 \\ K_{C2} = 1.922 \\ K_{C3} = 1.017 \\ \mathrm{We}_{cr} = 1.24 \end{cases} \tag{24}$$

$$\phi_n^{BK} = K_{B1}\frac{\alpha(1-\alpha)\varepsilon_l^{1/3}\exp\left(-\frac{\mathrm{We}_{cr}}{\mathrm{We}}\right)}{D_S^{11/3}\left[1+K_{B2}(1-\alpha)\sqrt{\frac{\mathrm{We}}{\mathrm{We}_{cr}}}\right]}, \qquad \begin{cases} K_{B1}=1.6 \\ K_{B2}=0.42 \end{cases} \tag{25}$$

1.3 Modelling of turbulence

The effective viscosity of the liquid phase is as follows,

$$\nu_l^{eff} = \nu_l + \nu_l^t, \tag{26}$$

where, it is assumed that the total turbulent viscosity ν_l^t is a superposition of the shear-induced turbulent viscosity and the bubble-induced turbulent viscosity as follows [11],

$$\nu_l^t = C_\mu \frac{k_l^2}{\varepsilon_l} + \frac{1}{2}C_{\mu b}D_S\alpha\left\|\vec{U}_g - \vec{U}_l\right\|, \qquad C_{\mu b}=0.6 \quad . \tag{27}$$

where k_l and ε_l are the turbulent kinetic energy and the turbulent dissipation rate respectively, calculated according to a classical single-phase k-ε model.

The effective viscosity of the gas phase can be assumed as a superposition of the gas molecular viscosity and the turbulent viscosity due to gas-liquid interactions. In present calculations a laminar flow was assumed for the gas phase.

2. Model validation

The present model has been validated against the DEDALE experiment [12], in which adiabatic air-water flow was tested in a vertical pipe made of methacrylate, with the inner diameter equal to 38.1 mm and with the total length equal to 6 m. The measurements were performed at three different axial locations: *y/D* = 8, 55 and 155. The first position (*y/D* = 8) was used as the inlet cross section in the calculations. Two experimental cases, DEDALE1101 and DEDALE1103, have been chosen for the validation. Table 1 contains the inlet conditions and Figs. 1 through 3 show the validation results for the two cases.

Table 1. Inlet conditions for validation cases DEDALE1101 and DEDALE1103 [12].

Property	DEDALE1101	DEDALE1103
Liquid superficial velocity, J_l [m/s]	0.877	0.877
Gas superficial velocity, J_g [m/s]	0.0588	0.1851
Void fraction, α [%]	4.8	15.2
Turbulence kinetic energy, k_l [m^2/s^2]	$4.23\cdot10^{-3}$	$1.78\cdot10^{-2}$
Interfacial area density, a_i [m^{-1}]	97	269

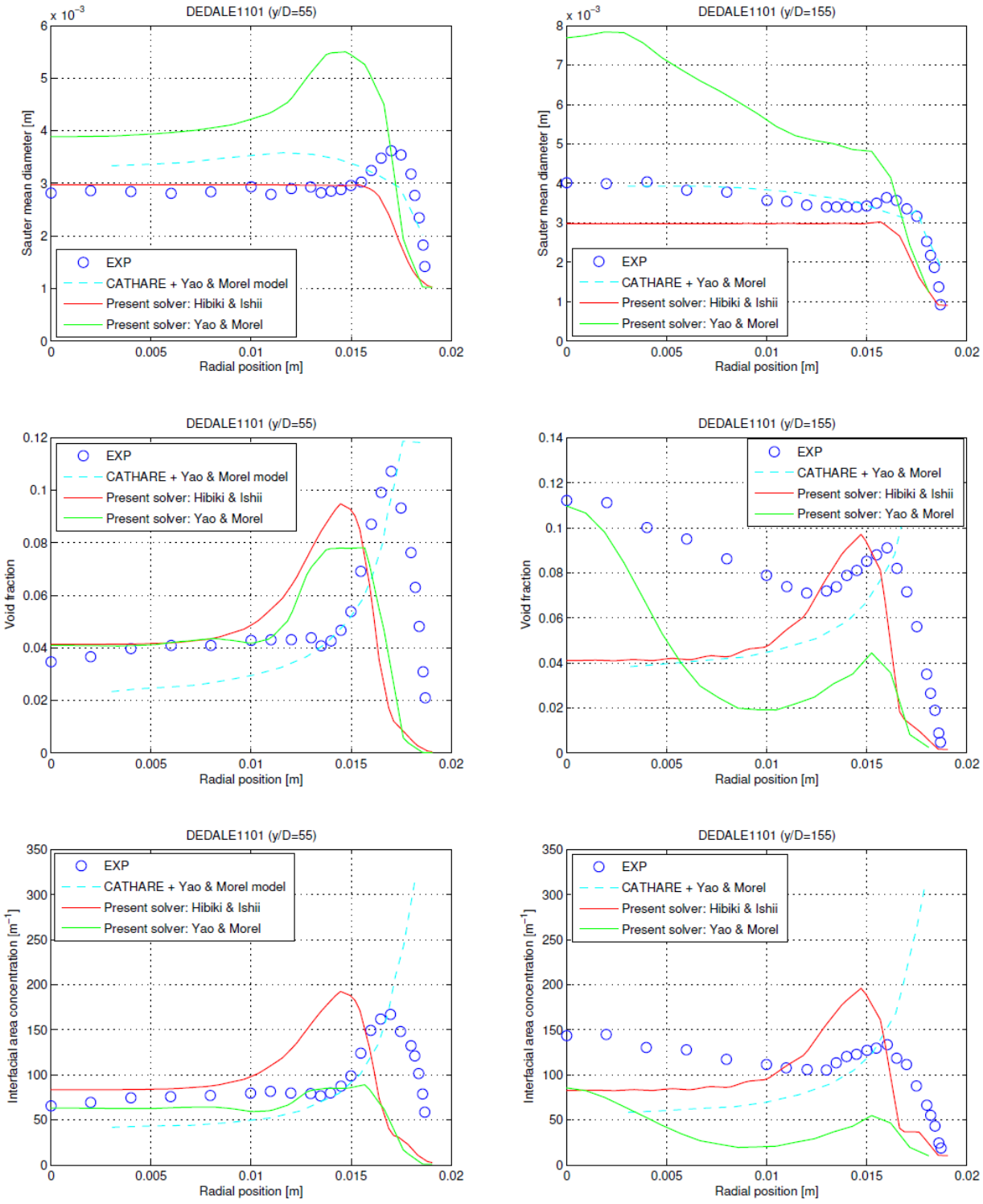

Figure 1. Comparisons of present predictions of bubble Sauter-mean diameter, void fraction and interfacial area concentration with experimental data [12] and predictions by CATHARE [10] obtained for the DEDALE1101 case.

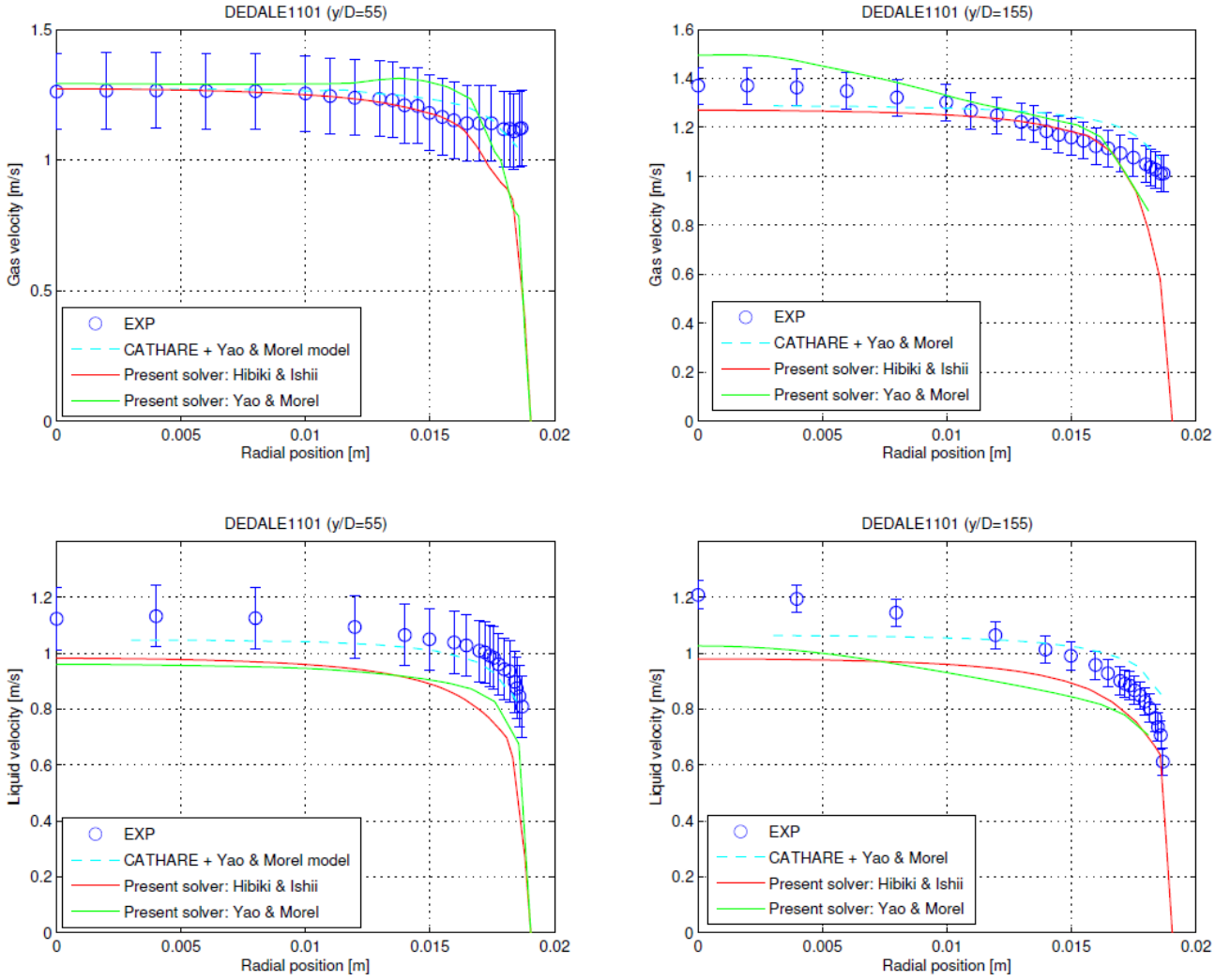

Figure 2. Comparisons of present predictions of gas and liquid velocities with experimental data [12] and predictions by CATHARE [10] obtained for the DEDALE1101 case.

As can be seen in Fig.1, the bubble Sauter-mean diameter is predicted correctly in the central part of the channel for *y/D* = 55. According to measurements, the diameter has a non-uniform distribution with maximum values about 3.5 mm close to the wall surface. This effect is not captured when employing the Hibiki & Ishii model for the bubble breakup and coalescence. The bubble size peaking effect is predicted with the Yao & Morel model; however, the bubble size is then larger than measured. The void fraction peaking observed at *y/D* = 55 has been captured very well by the present model, however, the void drift towards the channel centre observed at *y/D* = 155 is not captured when employing the Hibiki & Ishii model for the bubble breakup and coalescence. The gas velocities shown in Fig.2 are generally in good agreement with the measurements; however, liquid velocities tend to be under-predicted. A possible explanation is that the inlet mass flow rate specified in the present calculation is slightly lower than the one actually used in the experiments.

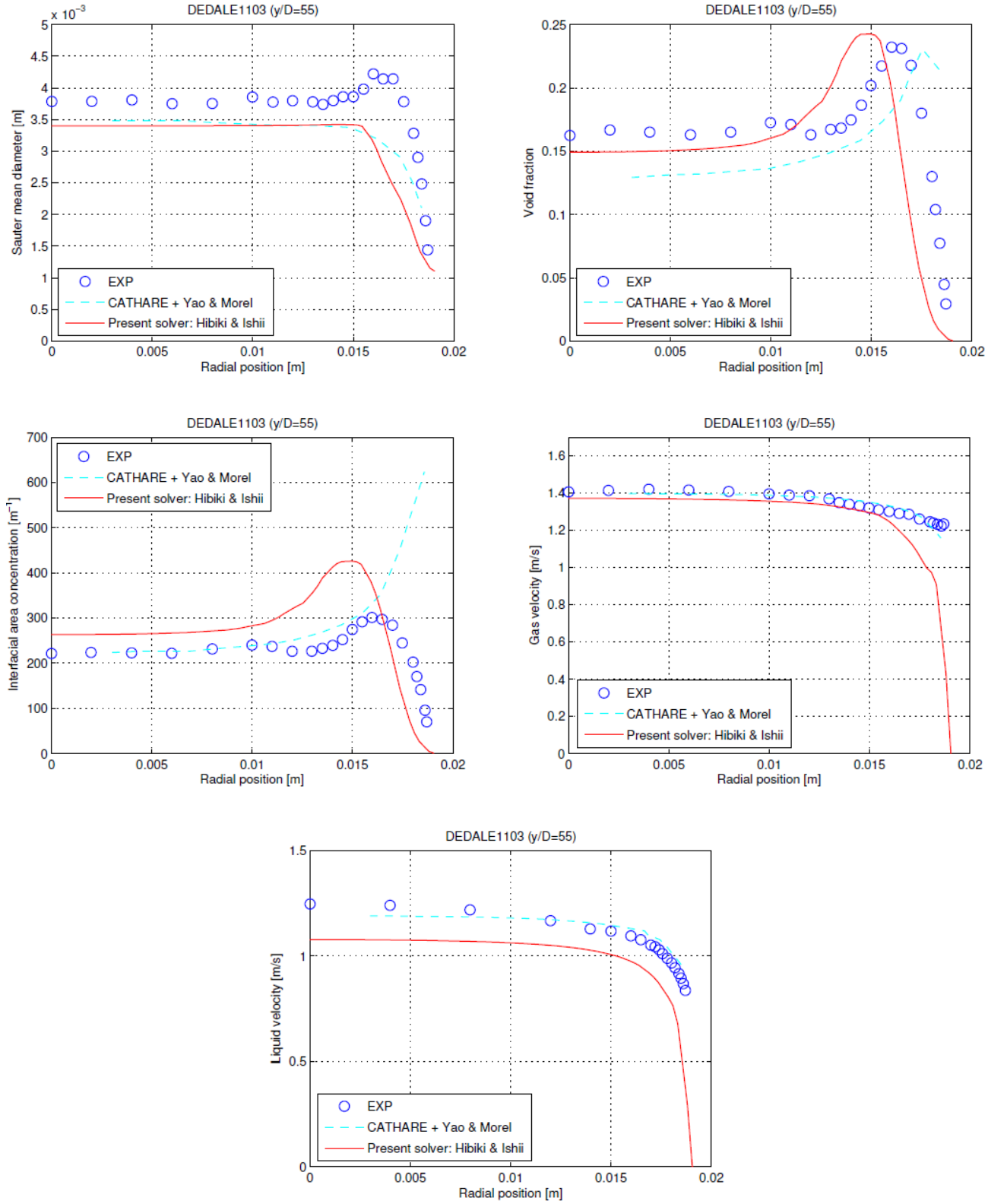

Figure 3. Comparisons of present predictions of bubble Sauter-mean diameter, void fraction, interfacial area concentration and phasic velocities with experimental data [12] and predictions by CATHARE [10] obtained for the DEDALE1103 case.

The results shown in Fig. 3 confirm that the present model predicts correctly the bubble size and void fraction distributions. In particular, the model predicts the void fraction peaking close to the wall. A similar discrepancy as for the DEDALE1101 case is observed for the liquid phase velocity.

3. Conclusion

A two-fluid adiabatic bubbly flow model has been implemented into the OpenFOAM solver. The model includes closure relationships for the interfacial momentum transfer for bubbles moving in a turbulent continuous liquid phase. Bubble size is predicted from the interfacial area concentration transport equations, including the source and sink terms resulting from the bubble coalescence and breakup. The present model has been validated against measurements performed in a vertical upflow of air-water in a non-heated pipe. It is concluded that the model predicts correctly the main features of the bubbly flow including the bubble size distribution and the void fraction distribution including the wall peaking effect. Further work is needed to improve the accuracy of the predictions, to extend the model to higher void fractions, as well as to include the heat and mass transfer effects.

4. References

[1] OpenCFD Limited, http://www.openfoam.com

[2] M. Ishii, *Thermo-fluid dynamic theory of two-phase flow*, Eyrolles, 1975.

[3] H. Rusche, "Computational fluid dynamics of dispersed two-phase flows at high phase fractions", PhD Thesis, Imperial College, London, 2002.

[4] M. Ishii and N. Zuber, "Drag coefficient and relative velocity in bubbly, droplet or particulate flow", *AIChE Journal*, Vol. 25, 1979, pp.843-855.

[5] D.A. Drew and R.T. Lahey, Jr., "The virtual mass and lift force on a sphere in rotating and straining inviscid flow", Int. J. Multiphase Flows, Vol. 13, 1987, pp. 113-121.

[6] A. Tomiyama, "Strugle with computational bubble dynamics", Third International Conference on Multiphase Flows, ICMF-3, 1998.

[7] A.D. Gosman et al., "Multidimensional modelling of turbulent two-phase flow in stirred vessels", AIChE Journal, Vol. 38, 1992, pp.1946-1956.

[8] N. Zuber, "On the dispersed two-phase flow in the laminar flow regime", *Chem. Eng. Sci.*, Vol. 19, No. 11, 1964, pp. 897-917.

[9] T. Hibiki and M. Ishii, "Development of one group interfacial area transport equation in bubbly flow systems", *Int. J. Heat Mass Transfer*, Vol. 45, 202, pp. 2351-2372.

[10] W. Yao and C. Morel, "Volumetric interfacial area prediction in upward bubbly two-phase flow", *Int. J. Heat and Mass Transfer*, Vol. 47, 2004, pp. 307-328.

[11] Y. Sato et al., "Momentum and heat transfer in two-phase bubbly flow", *Int. J. Multiphase Flows*, Vol. 7, 1981, pp. 167-178.

[12] D. Bestion and P. Peturand, "Review of the existing data basis for the validation of models for CHF", 6th EURATOM framework program NURESIM, 2006.